



ENHANCEMENT OF SHG IN FUSED SiO₂ BY CORONA POLING UNDER WATER, WATER VAPOR AND SALTY ENVIRONMENTS

Chun-An Tsai

Department of Electrical Engineering, National Taiwan Ocean University, Keelung, Taiwan, R.O.C.

Jung Ning Wang

Department of Electrical Engineering, National Taiwan Ocean University, Keelung, Taiwan, R.O.C.

Wei-Kuo Chao

Department of Electrical Engineering, National Taiwan Ocean University, Keelung, Taiwan, R.O.C.

Tsung Yuan Cheng

Department of Electrical Engineering, National Taiwan Ocean University, Keelung, Taiwan, R.O.C.

Wan-Rone Liou

Department of Electrical Engineering, National Taiwan Ocean University, Keelung, Taiwan, R.O.C.

See next page for additional authors

Follow this and additional works at: <https://jmstt.ntou.edu.tw/journal>



Part of the [Electrical and Computer Engineering Commons](#)

Recommended Citation

Tsai, Chun-An; Wang, Jung Ning; Chao, Wei-Kuo; Cheng, Tsung Yuan; Liou, Wan-Rone; and Wu, Adam Y. (2008) "ENHANCEMENT OF SHG IN FUSED SiO₂ BY CORONA POLING UNDER WATER, WATER VAPOR AND SALTY ENVIRONMENTS," *Journal of Marine Science and Technology*: Vol. 16: Iss. 2, Article 2.

DOI: 10.51400/2709-6998.2020

Available at: <https://jmstt.ntou.edu.tw/journal/vol16/iss2/2>

This Research Article is brought to you for free and open access by Journal of Marine Science and Technology. It has been accepted for inclusion in Journal of Marine Science and Technology by an authorized editor of Journal of Marine Science and Technology.

ENHANCEMENT OF SHG IN FUSED SiO₂ BY CORONA POLING UNDER WATER, WATER VAPOR AND SALTY ENVIRONMENTS

Authors

Chun-An Tsai, Jung Ning Wang, Wei-Kuo Chao, Tsung Yuan Cheng, Wan-Rone Liou, and Adam Y. Wu

ENHANCEMENT OF SHG IN FUSED SiO₂ BY CORONA POLING UNDER WATER, WATER VAPOR AND SALTY ENVIRONMENTS

Chun-An Tsai*, Jung Ning Wang*, Victor Chao-Wei-Kuo*, Tsung Yuan Cheng*,
Wan-Rone Liou* and Adam Y. Wu*

Key words: SHG, poled fused silica glass.

ABSTRACT

We found that optical nonlinearity in SiO₂ glass sample can be greatly enhanced when sample is poled in wet and salty environments, and the nonlinearity in the sample can be reduced drastically when sample is washed in water. Possible causes for the observed enhancement and reduction of optical nonlinearity in SiO₂ glass are discussed.

I. INTRODUCTION

In 1961, the second harmonic generation (SHG) experiment of Franken *et al.* [27] marked the birth of the field of nonlinear optics. They directed a ruby laser beam at 6942 Å through a quartz crystal and observed ultraviolet radiation from the crystal at 3471 Å. Second harmonic generation of electromagnetic waves at low frequencies have been known for a long time. Harmonic generation of optical waves follows the same principle and should also be observable. The linear and nonlinear effects depend on the interaction between input and output electric fields of light in material. Power generated at the second harmonic frequency increases as the square of the intensity of the applied laser light. Although nonlinear effects are small perturbations of linear process, requiring high field strength to observe, there are ways to obtain substantial conversion efficiencies in many nonlinear optical materials.

In 1991, second-harmonic generation (SHG) in poled fused silica was reported by Myers *et al.* [18]. The effect drew much interest because of a multitude of potential device applications. Such applications include devices for electro-optic switching, frequency doubling crystals, linear electro-optic modulation and frequency conversion, which can be integrated monolithically into optical fibers and planar integrated circuit geometry. It has been shown that a large second-order nonlinearity $\chi^{(2)}$ in

poled fused silica of 1 pm/V [18] can be induced in the near surface ($\sim 4 \mu m$) region of commercial fused-silica optical flats by poling process using electric field of $E \sim 5 \times 10^4 V/cm$ and temperature at 250°C~325°C [18].

In 1992, the values of second-order nonlinear coefficient d_{33} of the corona poled glass films are estimated to be 0.5 pm/V by Okada *et al.* [22]. The origin of the $\chi^{(2)}$ is considered to be related to the defects in the glass films. In 1993, the values of second-order nonlinear coefficient d_{33} of about 0.5 pm/V in corona poled Corning 7059 glass films was reported by Okada *et al.* [23]. Nasu *et al.* in 1995 [20] reported that the intensity of SHG was the largest when the glasses were poled at 3 kV and 200°C for 4 hours, and d_{33} was evaluated to be 0.37 pm/V. The d_{33} was evaluated to be 0.39 pm/V as reported by Henry *et al.* in 1995 [9]. In 1995, Lundquist *et al.* [14] reported SHG measurements on SiC films using pulsed laser ablation (PLA). d_{33} was found to be as large as 10 pm/V. In 1995, Henry *et al.* [10] observed optical nonlinearity in fused silica by proton implantation, averaged $\chi^{(2)}$ of the order of 1 pm/V was induced in low-water fused silica, with isolated regions exhibiting $\chi^{(2)}$ as large as 1.6 pm/V. In 1991, Harris *et al.* [8] reported the $\chi^{(2)}$ value of the effective second order nonlinear susceptibility for poled β -SiC to be $1.05 \pm 0.3 pm/V$.

In this paper, a corona poling process in fused silica samples under wet and salty environment at room temperature will be discussed. At a fixed poling field, we changed the temperature and water vapor conditions around the fused silica samples. We observed a large second harmonic generation from the samples. We observed that the nonlinearity in the poled sample can be reduced drastically by washing the samples in water. We found that the main cause of the nonlinearity resides not only inside the sample, but also resides mainly on the surface of the sample. We organize this paper in the following fashions: Section I is Introduction. In section II, we introduce the theoretical analysis. In section III, experimental procedure is discussed. The results and discussion of experiments are presented in section IV. The conclusion is given in section V.

Paper submitted 12/08/06; accepted 03/27/07. Author for correspondence:

Adam Y. Wu (e-mail: b0201@mail.sju.edu.tw).

* Department of Electrical Engineering, National Taiwan Ocean University, Keelung, Taiwan, R.O.C.

II. THEORETICAL ANALYSIS

1. Effect of Second Harmonic Generation in Fused Silica Glass by Corona Poling

It is generally known that the intensity of the SHG of corona poled glass depends on the applied poling electric field, poling time, poling temperature, ion concentration in the air, defects and impurities on the glass surface, defects and impurities in the sample, we will discuss these factors in the following sections.

1) The Space-Charge Model

In the poled fused silica experiments, Myers *et al.* [18] proposed that the SHG originated from a space-charge region created by migrating impurity ions and electrons. Under the action of voltage applied to heated glass, impurity ions will drift to cathode where most of them are neutralised by incoming electrons, leaving behind a negatively charged depletion region near anode surface (assuming zero ionic conductivity at the anode). A high electrostatic field will then appear in a depletion region just below the anode, peaking at the interface. Assuming that all the ions reaching the cathode are neutralised, it can be shown that in steady-state the electric field E_0 at the anode interface, and the depletion region width w , are given by [12]

$$E_0 = \frac{wqN_0}{\epsilon} \quad (1)$$

$$w = \sqrt{\frac{2\epsilon V_{app}}{qN_0}} \quad (2)$$

where N_0 is the number density of ions before poling, q is the electronic charge, ϵ is the dielectric permittivity, V_{app} is the applied voltage, and E_0 is the electric field inside sample.

2) Poling Time, Applied dc Field and Speed of Forming of Depletion Region

In 1975 Bethea [2] reported the nonlinear optical coefficient of the electric field induced second harmonic generation in glass. In 1996 Takebe *et al.* [26] reported the effective second-harmonic generation as a function of poling time and applied dc field. Two mechanisms have been proposed to explain the thermal poling phenomenon. One involves the orientation of bonds or dipoles and the other a frozen in electric space charge field. Both mechanisms predict the second-order nonlinearity (SON) to be proportional to the strength of the electrical field in the depletion region near the anode surface ($\chi_{22}^{(2)} \sim V/d$, where V is the applied voltage and d is the thickness of the poled region, i.e, the depletion region). By assuming that the pump beam propagates transversely to the poled region, the second-harmonic (SH) signal should therefore be proportional to the square of applied voltage [$P_{2\omega} \sim (\chi_{22}^{(2)} d)^2 \sim V^2$]. The speed of the formation of the depletion region is about several seconds as is determined by cationic conductivity of the glass. Kazansky and Russel [12] also reported that a frozen-in space charge field could cause the appearance of large quadratic nonlinearities in thermally poled glass (corona poled), which is obtained from experimental tests of the ratio of nonlinear tensor components

and the spatial distribution of the induced $\chi_{22}^{(2)}$. The components of the second harmonic polarization in a glass subjected to a dc electric fields are given by

$$P_z = \epsilon_0 d_{33} E_z^2 + \epsilon_0 d_{31} (E_x^2 + E_y^2) \quad (3)$$

$$P_y = 2 \epsilon_0 d_{31} E_y E_z \quad (4)$$

$$P_x = 2 \epsilon_0 d_{31} E_x E_z \quad (5)$$

3) Corona Poling in Polymer Films and Other Materials

Corona poling is a powerful method for creating a large potential across many polymer films [6]. It can orient the nonlinear optical dopants noncentrosymmetrically in polymer matrix and thus large SHG intensities can be obtained [6,7]. Ion penetration effect on surface space charge effects that occur at the film surface and in the bulk, and corona poling affecting the magnitude and the temporal stability of the SHG intensity, have been studied [6].

So far, many papers have used intense electric-field generated by a positive dc needle tip to change the ion orientation inside the sample [1,4,5,12,23,25,26]. This corona poling method provides not only large field on sample but also prevents any damage to sample surface due to physical contact. In such experiment a heater under the sample is commonly used to provide high temperature.

When heat is provided during corona poling, bond charges will be liberated and depletion region in the sample can be formed. In 1997 Aust *et al.* [1] performed an experiment by periodically poled a the Z-cut lithium niobate. The Maker Fringe scans taken before poling, it took about 30 minutes for temperature to cycle from 25°C to 200°C and back to 25°C. They spent 17 hours for the temperature cycle. After the experiment the sample was washed in water, they observed some thing interesting. There are some shifts in the Maker Fringes. It was first thought that these shifts are due to non-neutralized pyroelectric charge on the sample surface. Index changes due to a static electric field E^{stat} are given by

$$\Delta n_0 = -\frac{n_0^3}{2} r_{13} E_3^{\text{stat}} \quad (6)$$

where r_{13} is the linear electro-optic coefficient, E^{stat} is the static electric field, and n_0 is the index of refraction. However, calculation showed that magnitude of E^{stat} is -70kV/mm . They therefore believed that some other phenomenon, such as surface effects or impurity migration, is causing the large fringe shifts in their annealed and unwashed samples. Their results showed that the Maker fringe analysis is very sensitive to the processing history of the material. It is unclear whether the observed effects arise from surface or bulk artifacts.

Takebe *et al.* [26] used different poling atmosphere in air and vacuum. Their result indicates that some species in the air, such as hydrogen or oxygen ions, may be involved in the poling process. Their results demonstrated that the second harmonic generation is related to poling atmosphere [6,26].

In our experiments, we found that SHG changes greatly when fused silica glass sample was first poled and then treated under various conditions. When we poled silica sample, with water vapor around the sample surface at room temperature, large nonlinearity in glass appeared. We believe that a detailed study of corona poling processes under rich water environment can provide useful information concerning the nonlinear optical properties in fused SiO₂.

2. Maker Fringes

The refractive index of optical materials at frequency 2ω may be different from that at frequency ω . Because of this dispersion, waves propagate in material associated with these two refractive indices may have two different velocities:

$$C_1 = \frac{C_0}{n_1(\omega)} = \frac{\omega}{k_1} \quad (7)$$

$$C_2 = \frac{C_0}{n_2(2\omega)} = \frac{\omega}{k_2} \quad (8)$$

where C_0 is the light velocity in vacuum. $n_1(\omega)$ and $n_2(2\omega)$ are the refractive indices for ω and 2ω , C_1 and C_2 are the propagating phase velocities for ω and 2ω , respectively. k_1 and k_2 are the wave vectors of ordinary and extraordinary ray, respectively.

From the above equations we note that: Wave propagates in material associated with the larger refractive index will move slower. Maker Fringes may result because of the phase difference $\Delta k = |k_1 - k_2|$ between the fundamental and the second harmonic wave [24]. Because the two waves travel at different velocities, the phase between the SH at one point in the sample is not in phase with that generated at a particular point in the sample. The destructive interference between two wave occurs and the SH signal starts to decrease. The phase mismatch will cause the second harmonic to go through periods of constructive and destructive interference as it propagates through the nonlinear material, producing oscillations at a period of twice the coherence length, l_c . These are the Maker fringes [15].

Maker fringes utilize change of incident angle θ so that traveling distance of wave in sample can cause the phase difference Δk between ordinary ray and extraordinary ray to interfere with each other so that oscillations in intensity are observed. This oscillation can be expressed as $\sin^2 \phi$, and is related to the coherence length l_c through the following relations:

$$\sin^2 \phi = \sin^2 \left(\frac{\pi \ell}{2l_c(\theta)} \right) \quad (9)$$

$$l_c(\theta) = \frac{\lambda}{4|n_\omega \cos \theta_\omega - n_{2\omega} \cos \theta_{2\omega}|} \quad (10)$$

where l_c is the coherence length. ℓ is the thickness of sample. n_ω and $n_{2\omega}$ are the refractive indices of sample for

waves at frequency ω and 2ω , respectively. θ_ω and $\theta_{2\omega}$ are the refraction angles for waves with frequency ω and 2ω , respectively.

Maker fringes also figure a period between oscillations corresponding to twice the coherence length, $2l_c$. If the optical path length of the nonlinearity is greater than one coherence length as the sample is rotated, the signal would exhibit Maker fringes. When the distance is an odd multiple number of the coherence length as the laser light is passing through the sample, the largest maximum intensity of SHG will be observed. In opposition, if the distance is an even multiple number of the coherence length, the intensity would be minimum.

3. Calculation for d_{ij} Values

Analyzing Maker fringes is a common method for researchers to obtain NLO coefficients of unknown samples. However, in order to obtain accurate value, a known reference value is usually used. For examples, reference values such as d_{11} in quartz, d_{36} in ADP, d_{36} in KDP, can be used [16].

According to reference [11], the formula for the intensity of the second harmonic can be written as:

$$I_{2\omega} = \frac{512 \pi^3}{A} \times d^2 \times t_\omega^4 \times T_{2\omega}^2 \times I_\omega^2 \times \frac{\sin^2 \phi}{(n_\omega^2 - n_{2\omega}^2)^2} \quad (11)$$

$$\phi = \left(\frac{\pi \ell}{2} \right) \left(\frac{4}{\lambda} \right) (n_\omega \cos \theta_\omega - n_{2\omega} \cos \theta_{2\omega}) \quad (12)$$

where: $I_{2\omega}$ is the intensity of SHG. A is the laser beam area. d is the nonlinear optical coefficient. t_ω is the transmission factor at ω . $T_{2\omega}$ is the transmission factor at 2ω . θ is rotation angle. I_ω is the intensity of fundamental beam. n_ω is the refractive index at ω . $n_{2\omega}$ is the refractive index at 2ω . ℓ is sample thickness. λ is wavelength of the fundamental beam in air.

We can obtain the second order nonlinear optical susceptibility tensor matrix and fundamental wave in quartz as follows:

$$\begin{bmatrix} P_x \\ P_y \\ P_z \end{bmatrix} = \begin{bmatrix} d_{11} & -d_{11} & 0 & d_{14} & 0 & 0 \\ 0 & 0 & 0 & 0 & -d_{14} & -d_{11} \\ 0 & 0 & 0 & 0 & 0 & 0 \end{bmatrix} \begin{bmatrix} E_x^2 \\ E_y^2 \\ E_z^2 \\ 2E_x E_y \\ 2E_z E_x \\ 2E_x E_y \end{bmatrix} \quad (13)$$

Expanding equation (13) we obtain:

$$\begin{aligned} P_x &= d_{11} E_x^2 - d_{11} E_y^2 + 2d_{14} E_z E_y \\ P_y &= -2d_{11} E_x E_y - 2d_{14} E_z E_x \\ P_z &= 0 \end{aligned} \quad (14)$$

According to the Kleinmann symmetry, $d_{14} = 0$ in quartz crystal [11,13] and d_{11} is a positive value [4]. If we want to measure the d_{11} of a y-cut quartz, the rotation axis should be the

c-axis and the fundamental and extraordinary ray should both be P-waves. In such case, equation (14), becomes

$$P_x = d_{11} E_x^2 \quad (15)$$

From (11), we have: [11]

$$t_\omega = \frac{2 \cos \theta}{n_\omega \cos \theta_\omega + \cos \theta} \quad (16)$$

$$\begin{aligned} T_{2\omega} &= 2 \cos \theta_{2\omega} \cdot n_{2\omega} \cdot (\cos \theta + n_\omega \cos \theta_\omega) \cdot \\ &(n_\omega \cos \theta_\omega + n_{2\omega} \cos \theta_{2\omega}) \div (n_{2\omega} \cos \theta_{2\omega} + \cos \theta)^3 \\ &= 1.72 \end{aligned} \quad (17)$$

where $n_\omega = 1.53413$ and $n_{2\omega} = 1.54702$ in quartz [11]. From experimental result we can choose the SHG intensity at a particular angle θ , and from the Snell's law, we have:

$$\sin \theta_\omega = \frac{\sin \theta}{n_\omega} \quad (18)$$

$$\theta_\omega = \sin^{-1} \left(\frac{\sin \theta}{n_\omega} \right) \quad (19)$$

$$\theta_{2\omega} = \sin^{-1} \left(\frac{\sin \theta}{n_{2\omega}} \right) \quad (20)$$

From (11) to (20) we can obtain the relative d_{ij} value of unknown samples with respect to that of quartz.

III. EXPERIMENTAL PROCEDURE

1. Samples

Quartz crystal is purchased from the Entrust SLEO Photonics Co., Ltd. The Y-cut (010) sample has dimensions $10\text{mm} \times 10\text{mm} \times 3\text{mm}$. According to the SLEO Photonics Co., Ltd. the crystal quartz samples are produced by method of hydrothermal process. Hydrothermal process is a method imitates nature crystal growth. SiO₂ raw material was first melted at high temperature and then crystallized upon cooling on a seed plate of quartz single crystal. Proper-size crystals so grown are then collected. Because quartz concentration in melted solution is low in natural environment, it needs a long time for quartz to crystallize. Artificially, one can increase the concentration of SiO₂ in solution to reduce the crystalline time in laboratory.

Silica glass plates were purchased from the Heraeus Company of America. The specifications are Optosil I or Optosil II. The fabrication of glass is like this: First, crystal quartz is melted into molten form above 1750°C in a furnace and then is cooled down slowly to form glass at low temperature.

2. Instrument

We used a Model VC-50 diamond cutter purchased from the Leco Instrument Taiwan Ltd. to cut our samples. The diamond blade is 4" in diameter with a 0.5" arbor hole and 0.012" in thickness. The sample wafers were cut into proper sizes. We used mesh 1000 waterproof abrasive paper to polish the cut faces.

We used a Quanta-Ray GCR-200 Nd:YAG laser manufac-

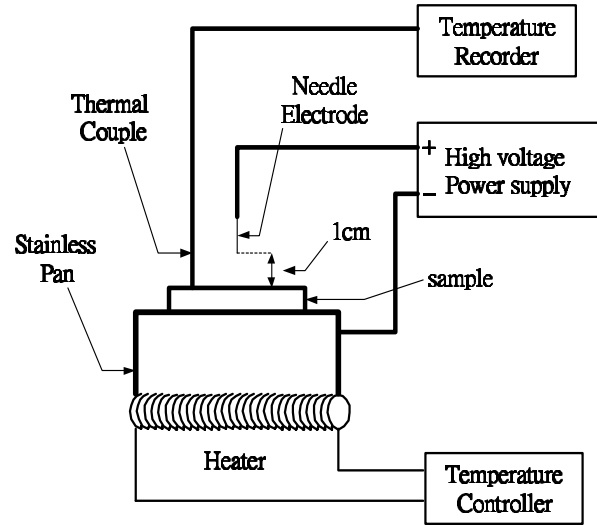


Fig. 1. The diagram of arrangement for the corona poling.

tured by the Spectral Physics Company. It's specifications are as follows:

Wavelength	1064nm
Repetition Rate	10Hz
Energy	Q-Switch 1250mJ
Pulse duration	8~9 ns
Beam diameter	6mm

The PMT and the amplifier we used were both manufactured by the Hamamatsu Company. The model of PMT is R636 and the spectral response range is from 185 to 930nm . The model of amplifier is C5594. It has a wide frequency bandwidth from 50KHz ~ 1.5GHz and a high gain of 36dB . It requires an applied bias voltage of $+12$ ~ $+16\text{V}$.

The oscilloscope we used was manufactured by the Tektronix Company manufactured, its model is TDS620A, and its triggering frequency can reach 500MHz . The Boxcar integrator was manufactured by the Stanford Research System Company, the model is System SR250. Its gate width can reach 1ns .

3. Methods for Conventional Corona Poling

In order to break the centrosymmetry in glass sample, we utilized the gas molecules surrounding the sample and the original molecules inside the sample ionized by heating and oriented by a high electric field. The experimental setup for corona poling is shown in Fig. 1. We used a thermocouple to monitor the temperature by a voltage meter. We controlled and kept the temperature of the sample at about 270°C [14,18,19,23]. A positive 4900V (with a small corona dc current of less than 0.1mA) was applied to a positive needle tip placed about 1cm above the sample. During the poling process, the temperature of the sample was kept at 270°C , and the voltage was kept at 4900V . The poling time was 270 minutes. Temperature was then reduced to room temperature with the electric field still applied.

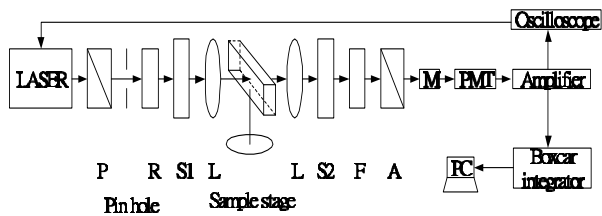


Fig. 2. The experiment setup. LASER is Nd: YAG laser. P is polarizer. R is half-wave retardation. S1 and S2 is harmonic separator for 1064 nm and 532 nm, respectively. L is lens (focal length 150 mm). F is high power filter. A is analyzer. M is monochromator. PMT is photo-multiplier tube.

As the sample was cooled down, the molecules in the sample remained in an oriented state as the material in the sample became thermally stable.

4. Experimental Setup

As shown in Fig. 2, a Q-switched Nd: YAG laser radiation of wavelength $1.064 \mu m$ was used. A high energy laser polarizer was used to differentiate polarization of the incoming beam. We define that wave is p-polarized when the polarization is parallel to the surface of our optical table, and s-polarized wave is the wave with the polarization perpendicular to the surface of the optical table. The angle between the normal of the polarizer and incident beam is 57° . The beam passing through the polarizer is p-polarized (96%) and the beam reflected from the polarizer s-polarized (99%). We chose the purer s-polarized wave as incident beam. Before the incident beam entering the system, it passed a 6mm-diameter hole made of steel to reduce the diameter of the beam and to make the beam cleaner and Gaussian like. The incident beam then passed through a $\lambda/2$ plate (multiple order of half wave retardation plate) for selecting s or p polarization.

After the $\lambda/2$ plate, we used a high energy laser harmonic separator for the 1064nm radiation (Transmission > 99.5%) to make sure that the incident beam entering the sample was pure 1064nm radiation. Because the sample thickness was only 1mm~2mm, we utilized a convex lens with a focal length of 150mm to focus the laser beam onto the sample surface. Sample was placed at the center of a rotational stage near the focal point of the beam. The diameter of the beam at sample was smaller than 1mm. The incremental step of the rotational stage was controlled to 0.01° .

A parallel light passes through a convex lens will be focalized. When this focalized light passes through the focal point it will start to diverge, we added another convex lens with the incident beam enters a non-centrosymmetri same focal length as the previous one. When the c sample a new frequency which doubles the original one will be generated. In order to measure the pure intensity of frequency-doubled light, we used two different filters, one is a KG3 Schott Glass filter for passing wavelength at 532nm (the product number is 03FCG167) and another is a high energy laser harmonic separator for 532nm (Transmission > 99.5%). The bandpass specification is $532 \pm 150nm$ for the

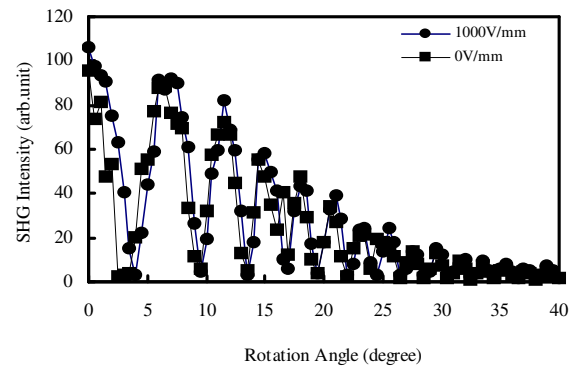


Fig. 3. The Maker Fringes of X-cut LiNbO₃. The sample width is 2mm, the rotational axis and the electric field are parallel to Z axis in the P-P mode, electric field is 1000V/mm.

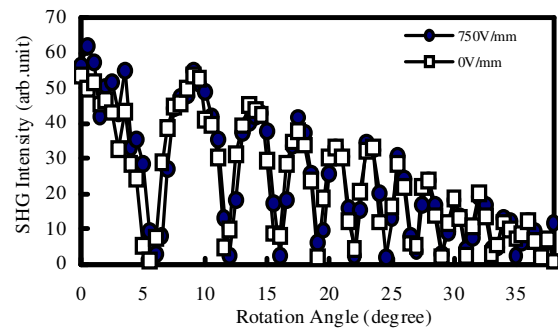


Fig. 4. The Maker Fringes of X-cut LiNbO₃. The sample width is 2mm, the rotational axis and the electric field are parallel to Z axis in the P-P mode, electric field is 750V/mm.

Schott Glass filter and is $532 \pm 50nm$ for the separator. These two filters can reduce all nongreen light to zero.

After the two filters, we used an analyzer to select the polarization of the second harmonic signal. The frequency-doubled 532nm radiation entered a SPEX monochromator for selecting the 532nm radiation. Signal was measured by a Hamamatsu R636 photomultiplier tube (PMT). Signal detected by the PMT and was further amplified by an amplifier of 36 dB. The signal was monitored by an oscilloscope and a boxcar integrator using 50Ω BNC cables. We utilized the oscilloscope to observe the waveform of the SHG and the boxcar integrator to filtrate out the noise and retain only the signal. The experimental setup is shown in Fig. 2.

5. Experimental Measurement

SiO₂ glass samples were used in this experiment. Y-cut quartz sample of 3mm thick was used as reference. Before each experiment, we measured the background for the experiment. After the experiment was done, the reference sample was removed and the real sample was inserted for measurement. Each data point was the average of five or more data readings. The noise to signal ratio was kept below 3%.

We used an X-cut LiNbO₃ crystal of 1mm thick to check if our experiment system was correct. In the test experiment of the

X-cut LiNbO₃ crystal, we applied the electric field along the Z-direction of the crystal. We measured the signals both in applied electric field and in zero field under the same conditions and obtained Fig. 3 and Fig. 4. These Figures indicate that our experiments can easily detect small oscillations of the Maker Fringes.

In this test experiment, the LiNbO₃ was cleaned with acetone ((CH₃)₂CO m.w.=58.08 g/mole) and methyl alcohol (CH₃OH). When the sample was dried, we painted Ag paste on the cut-faces of the sample uniformly and carefully. Then sample was baked in an oven so that moisture and organic material in the paint were driven away.

We utilized the corona poling to orient the surrounding molecules on the glass sample surface and the original molecules inside the glass sample. The corona poling process broke the centrosymmetry of the sample. In order to study the H₂O and salt effects in SHG, we have studied the SHG as a function of rotation angle (Maker fringes) in the samples prepared by the four poling methods under water and salt water environments as mentioned before. The conditions for these procedures are listed in Table 1.

IV. RESULTS AND DISCUSSION

In this section, we will use d_{ij} instead of $\chi^{(2)}$ for detailed experimental interpretations of our results. The simple relation between $\chi^{(2)}$ and d_{ij} is simply $\chi^{(2)} = 2d_{ij}$ [17,27]. We will discuss the enhancement of SHG in fused SiO₂ by corona poling under different environments. Since glass with a centrosymmetric structure can not be used to generate second-harmonic generation. Corona poling allows the localized hyperpolarizability to constructively interfere on the anode side of sample, forming a non-zero macroscopic susceptibility. The polarization of dipole moment is perpendicular to the sample surface, which is the preferred z-axis. If we ignore the components induced by the angle variation of the y-axis, the relation between second-order nonlinear susceptibility matrix and fundamental wave in poled glass can be expressed as follows:

$$\begin{bmatrix} P_x \\ P_y \\ P_z \end{bmatrix} = \begin{bmatrix} 0 & 0 & 0 & 0 & d_{15} & 0 \\ 0 & 0 & 0 & d_{15} & 0 & 0 \\ d_{31} & d_{31} & d_{33} & 0 & 0 & 0 \end{bmatrix} \begin{bmatrix} E_x^2 \\ E_y^2 \\ E_z^2 \\ 2E_y E_z \\ 2E_z E_x \\ 2E_x E_y \end{bmatrix} \quad (21)$$

When the Kleinmann symmetry holds, i.e. when the optical frequencies are within the transparency range of the medium, as is true with glass in visible region, we have $d_{15} = d_{31}$ [12]. For material with a single axis of symmetry and an effective $\chi^{(2)}$ created by corona poling, the additional symmetry condition of $d_{33} = 3d_{31}$ also exists [9,12,22]. From (21) we have:

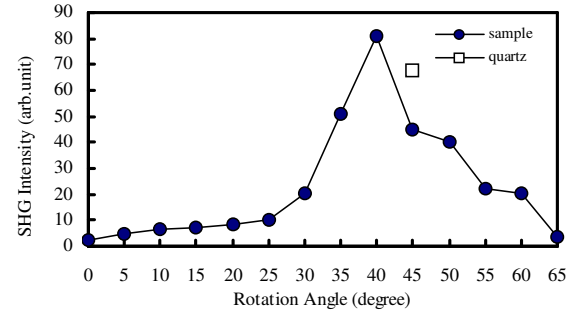


Fig. 5. The intensity of SHG as a function of rotation angle θ for a corona poled glass sample.

$$\begin{aligned} P_x &= 2d_{31}E_x(\omega)E_z(\omega), \\ P_y &= 2d_{31}E_y(\omega)E_z(\omega), \\ P_z &= d_{31}(E_x^2(\omega) + E_y^2(\omega)) + d_{33}E_z^2(\omega). \end{aligned} \quad (22)$$

The main purpose of this paper is to measure the electric field induced second harmonic generation in SiO₂ glass. Four methods for generating electric field in glass were used: 1) We used the standard corona poling at 270^oC as reported by other researchers [18,19] and measured the intensity of SHG as a function of rotation angle. 2) We used the corona poling method with the assistance of water vapor around the sample. 3) We used the corona poling method with water drops placed on the sample surface at room temperature. 4) We used the corona poling method at the room temperature with some salty water drops placed on the sample surface at room temperature. The conditions for each experiment are shown in Table 1.

1. NLO Effect in SiO₂ Glass by Corona Poling at 270^oC

In this section, we performed a similar corona poling experiment of SiO₂ at 270^oC as reported by other researchers [18,19] and used the Maker Fringes equation to calculate d_{eff} (See Appendix-B) and d^*_{eff} (See Table 3). After the poling experiment the sample was washed in water. We note here that Aust *et al.* had washed their lithium niobate sample in water after poling [1]. Since the sign of d_{eff} and d^*_{eff} could not be determined directly in our experiment, the values of d_{eff} and d^*_{eff} are absolute values.

The corona poling conditions are as follows: 1) The distance between the sample and the positive electrode needle tip is 1cm. 2) The poling voltage is 4900V. (3) The temperature is about 270^oC. 4) The poling duration is about 270 minutes. These poling conditions are the same as those published before and are shown in Table 1. [3,8,9,10,12,14,19,20,21,22,23]

Fig. 5 shows the intensity of SHG as a function of rotation angle θ for a corona poled glass sample. Fig. 5 shows the results in the P-P mode. We chose the value of $I_{2\omega} = 80.8$ (relative arbitrary unit) at $\theta = 40^o$ as a reference point in this sample. In order to find the d_{eff} value, we have to obtain all required parameters before substituting them into (11).

We chose the following known or measured values for further calculation:

For Fig. 5, case1: Parameters for glass sample, in the P-P mode:

$$\begin{aligned}\theta &= 40^\circ, \\ I_{2\omega} &= 80.8, \\ n_\omega(1.064\mu\text{m}) &= 1.45, \\ n_{2\omega}(0.532\mu\text{m}) &= 1.46 \text{ [19]},\end{aligned}$$

Using the Snell's law we obtain the refraction angles for θ_ω and $\theta_{2\omega}$ as follows:

$$\begin{aligned}\sin\theta &= n_\omega \sin\theta_\omega, \\ \theta_\omega &= \sin^{-1}\left(\frac{\sin\theta}{n_\omega}\right) = 26.31^\circ, \\ \sin\theta &= n_{2\omega} \sin\theta_{2\omega}, \theta_{2\omega} = \sin^{-1}\left(\frac{\sin\theta}{n_{2\omega}}\right) = 26.12^\circ,\end{aligned}$$

The transmission factors for the fundamental beam and frequency-doubled beam are:

$$t_\omega = \frac{2 \cos\theta}{n_\omega \cos\theta_\omega + \cos\theta} = 0.74,$$

$$\begin{aligned}T_{2\omega} &= 2 \cos\theta_{2\omega} \cdot n_{2\omega} \cdot (\cos\theta + n_\omega \cos\theta_\omega) \cdot \\ & (n_\omega \cos\theta_\omega + n_{2\omega} \cos\theta_{2\omega}) \div (n_{2\omega} \cos\theta_{2\omega} + \cos\theta)^3 \\ &= 1.58\end{aligned}$$

the coherence length is:

$$\begin{aligned}l_c &= \frac{\lambda}{4|n_\omega \cos\theta_\omega - n_{2\omega} \cos\theta_{2\omega}|} = 23.8\mu\text{m}, \\ \sin^2\phi &= \sin^2\left(\frac{\pi l}{2l_c}\right) = 0.038.\end{aligned}$$

By substituting the above parameters into (11) we obtain:

$$\frac{I_{2\omega}}{I_\omega^2} = \frac{512\pi^3}{A} \times d_{\text{eff}}^2 \times 34.03. \quad (23)$$

Using similar steps and methods, we chose $I_{2\omega} = 68.1$ (relative arbitrary unit) at $\theta = 45^\circ$ in Fig. 5 as reference point for quartz reference crystal, and obtain the following parameters:

For Fig. 5, case 2: parameters for quartz reference sample, in the P-P mode:

$$\theta = 45^\circ,$$

$$I_{2\omega} = 68.1,$$

$$d = 0.5 \text{ [3,4]},$$

$$n_\omega(1.064\mu\text{m}) = 1.53413,$$

$$n_{2\omega}(0.532\mu\text{m}) = 1.54702 \text{ [11]},$$

$$\sin\theta = n_\omega \sin\theta_\omega,$$

$$\theta_\omega = \sin^{-1}\left(\frac{\sin\theta}{n_\omega}\right) = 27.45^\circ,$$

$$\sin\theta = n_{2\omega} \sin\theta_{2\omega}, \theta_{2\omega} = \sin^{-1}\left(\frac{\sin\theta}{n_{2\omega}}\right) = 27.20^\circ,$$

$$t_\omega = \frac{2 \cos\theta}{n_\omega \cos\theta_\omega + \cos\theta} = 0.68,$$

$$\begin{aligned}T_{2\omega} &= 2 \cos\theta_{2\omega} \cdot n_{2\omega} \cdot (\cos\theta + n_\omega \cos\theta_\omega) \cdot \\ & (n_\omega \cos\theta_\omega + n_{2\omega} \cos\theta_{2\omega}) \div (n_{2\omega} \cos\theta_{2\omega} + \cos\theta)^3, \\ &= 1.72\end{aligned}$$

$$l_c = \frac{\lambda}{4|n_\omega \cos\theta_\omega - n_{2\omega} \cos\theta_{2\omega}|} = 18.33\mu\text{m},$$

$$\sin^2\phi = \sin^2\left(\frac{\pi l}{2l_c}\right) = 0.25.$$

Substituting the above parameters into (11) and using (24) we obtain:

$$\frac{I_{2\omega}}{I_\omega^2} = \frac{512 \pi^3}{A} \times 25.094 \times d_{11}^2 \quad (24)$$

Because we could not directly measure the thickness of the depletion layer on the anode side of poled sample, three possible thicknesses of the depletion layer of $3\mu\text{m}$, $5\mu\text{m}$ and $10\mu\text{m}$ [14] were used. By dividing (24) with (23) to obtain d_{eff} with different thicknesses, (23) can be expressed as follows:

$$\begin{aligned}\text{when } l &= 3\mu\text{m}, & \frac{I_{2\omega}}{I_\omega^2} &= \frac{512\pi^3}{A} \times d_{\text{eff}}^2 \times 34.03, \\ d_{\text{eff}} &= 0.94 \text{ pm/V}, \\ \text{when } l &= 5\mu\text{m}, & \frac{I_{2\omega}}{I_\omega^2} &= \frac{512\pi^3}{A} \times d_{\text{eff}}^2 \times 92.37, \\ d_{\text{eff}} &= 0.57 \text{ pm/V}, \\ \text{when } l &= 10\mu\text{m}, & \frac{I_{2\omega}}{I_\omega^2} &= \frac{512\pi^3}{A} \times d_{\text{eff}}^2 \times 330.88, \\ d_{\text{eff}} &= 0.29 \text{ pm/V}.\end{aligned}$$

There is only one peak in Fig. 5. This is because the nonlinear thickness $l = 3 \sim 10\mu\text{m}$ is smaller than the coherence length

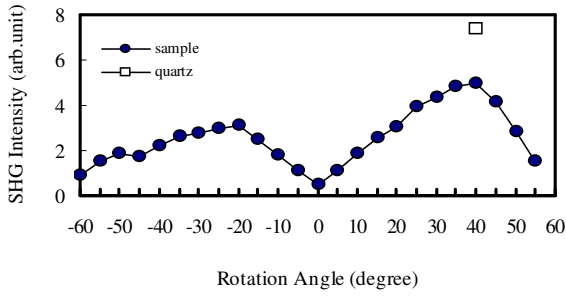


Fig. 6. After washing the poled sample for the P-P mode.

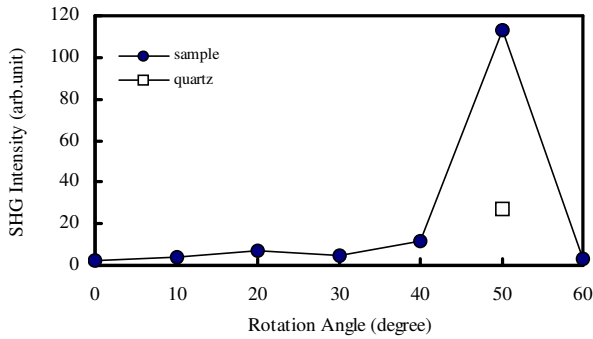


Fig. 7. The NLO effect on glass under corona poling. The poling conditions are 4900V, 270°C, 270 minutes, water on the sample, P-P mode.

$l_c = 23.8\mu\text{m}$. Hence, we have to increase the optical path length in the sample by rotating the sample. When the sample rotation angle reached 40 degree, the intensity of SHG became maximum. At this angle, the optical path length of the laser beam passing through the sample is just one coherence length.

By comparing with Fig. 5, it is clear that if we assume that the thickness of the nonlinear region in glass is $5\mu\text{m}$, the calculated d_{eff} value of the poled glass of 0.56 pm/V is already larger than the d_{11} of quartz crystal, which is 0.5 pm/V .

We then used water to wash the poled sample, the results for the P-P mode are shown in Fig. 6. We can see from Fig. 6 the SHG intensity decreases dramatically. This leads us immediately to believe that the nonlinearity maybe due to some residual nonlinear region on the glass surface.

For calculation, we chose the value $I_{2\omega} = 5$ at $\theta = 40^\circ$ as shown in the figure. In order to find the d_{eff} value, we have to obtain all required parameters before substituting them into (11). The results are:

$$\text{when } l = 3\mu\text{m} \text{ , } \frac{I_{2\omega}}{I_\omega^2} = \frac{512\pi^3}{A} \times d_{\text{eff}}^2 \times 22.80 \text{ ,}$$

$$d_{\text{eff}} = 0.076\text{ pm/V} \text{ ,}$$

$$\text{when } l = 5\mu\text{m} \text{ , } \frac{I_{2\omega}}{I_\omega^2} = \frac{512\pi^3}{A} \times d_{\text{eff}}^2 \times 61.87 \text{ ,}$$

$$d_{\text{eff}} = 0.046\text{ pm/V} \text{ ,}$$

$$\text{when } l = 10\mu\text{m} \text{ , } \frac{I_{2\omega}}{I_\omega^2} = \frac{512\pi^3}{A} \times d_{\text{eff}}^2 \times 221.64 \text{ ,}$$

$$d_{\text{eff}} = 0.024\text{ pm/V} \text{ .}$$

when we assume $l = 3\mu\text{m}$, we also found d_{eff}^* is 0.101 pm/V (See Table 3).

From these two experiments on unwashed and washed sample, we discovered that when the corona poled sample was washed by water; its SHG intensity decreases drastically. We believe that this phenomenon is related to some interaction between water and SiO₂ under high electric field. It is possible that a thin new chemical compound such as SiOH or other material is formed on the glass surface. The following experiment was performed to clarify this situation.

In our next experiment, we change some conditions. We put several water drops on the surface of glass sample and performed the corona poling at 270°C. The results are shown in Fig. 7. Again, if we assume that the thickness of the depletion layer is $3\mu\text{m}$, $5\mu\text{m}$ or $10\mu\text{m}$ [14,19] we obtain

$$\text{when } l = 3\mu\text{m} \text{ , } \frac{I_{2\omega}}{I_\omega^2} = \frac{512\pi^3}{A} \times d_{\text{eff}}^2 \times 20.22 \text{ ,}$$

$$d_{\text{eff}} = 2.08\text{ pm/V} \text{ ,}$$

$$\text{when } l = 5\mu\text{m} \text{ , } \frac{I_{2\omega}}{I_\omega^2} = \frac{512\pi^3}{A} \times d_{\text{eff}}^2 \times 54.75 \text{ ,}$$

$$d_{\text{eff}} = 1.27\text{ pm/V} \text{ ,}$$

$$\text{when } l = 10\mu\text{m} \text{ , } \frac{I_{2\omega}}{I_\omega^2} = \frac{512\pi^3}{A} \times d_{\text{eff}}^2 \times 193.62 \text{ ,}$$

$$d_{\text{eff}} = 0.67\text{ pm/V} \text{ .}$$

When we assume $l = 3\mu\text{m}$, we found that d_{eff}^* is 1.16 pm/V (See Table 3).

It is clear that d is more than two times as large as in the previous results, and that water can increase the nonlinear intensity. In Figs. 5, 6 and 7, we used (11) and calculated the intensity. The results are listed in Table 2. From Table 2 we can see that nonlinearity can be enhanced by water drop experiment and bleached by washing experiment. From Figs. 5 and 7 we can see that d_{eff} are 0.95 pm/V and 2.08 pm/V , respectively. From Figs. 5 and 7 we can also see that d_{eff}^* are 0.95 pm/V and 1.16 pm/V , respectively. This proves that glass indeed reacted with water in the corona poling process. Next, we want to know the relation between the poling time and SHG intensity.

2. Time Duration for Corona Poling at 270°C

In 1995 Myers *et al.* [19] reported effect of SHG in glass by changing the poling time and applied voltage. In 1996, Takebe *et al.* [26] also reported similar experiment. In this section, we want to know the relation between the SHG intensity and the poling time.

In this experiment the new conditions are that the time for poling was 180 minutes and we placed the water drops on the surface of the glass sample at 270°C. The result is shown in the Fig. 4.3a. The calculated coherence length is $23.2\mu\text{m}$, If we

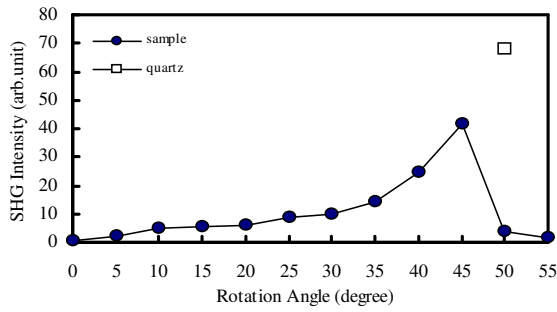


Fig. 8. The NLO effect of glass under corona poling. The poling conditions are 4900V, 270°C, 180minrtes, water on the sample, P-P mode.

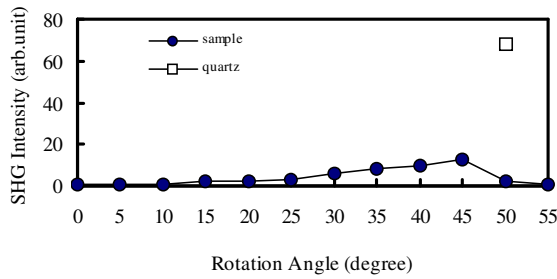


Fig. 9. Experimental results for sample shown in Figure 8 washed by water.

assume the nonlinear region is about $3\mu m$, d_{eff} is calculated to be $0.71pm/V$ (See Table 2), and d^*_{eff} is calculated to be $0.64pm/V$ (See Table 3).

From Figs. 7 and 8, we can see that the SHG intensity increases as the poling time increases. The results for the sample washed in water are shown in Fig. 9. We found that d_{eff} decreases from $0.71 pm/V$ to $0.42 pm/V$ and d^*_{eff} decreases from $0.64 pm/V$ to $0.42 pm/V$. As is clearly shown, after the sample was washed in water, the nonlinear optic coefficient decreased drastically.

3. NLO Effect in SiO₂ Glass by Corona Poling under Wet Environment at Room Temperature

In this section, our new conditions are the temperature was room temperature and water drops were placed on the sample surface. The results are shown in Fig. 10. The calculated d_{eff} for the $3\mu m$ thick case is $1.33pm/V$ and d^*_{eff} is $1.47pm/V$.

This result is interesting. From Figs. 7 and 10, we can see that d_{eff} are $2.08 pm/V$ and $1.33 pm/V$, respectively. From Figs. 5 and 10, we can see that d_{eff} are $0.95 pm/V$ and $1.33 pm/V$, respectively. It is clear that the SHG intensity is dependent more on water and less on temperature.

After the sample was washed by water the results are shown in Fig. 11. Again our calculations showed that d_{eff} is $0.31pm/V$ and d^*_{eff} is $0.26pm/V$. From Figs. 9 and 11, we can see that d_{eff} are $0.42 pm/V$ and $0.31 pm/V$, respectively. It appears that SHG intensity was caused essentially by material formed on the glass surface when experiment was performed at room temperature.

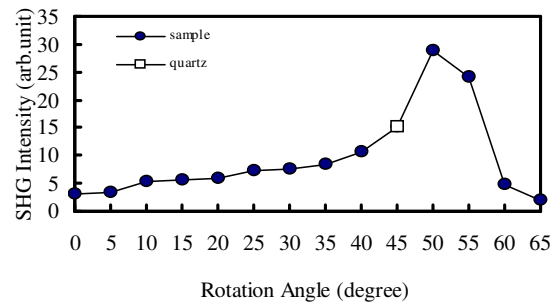


Fig. 10. The NLO effect of glass under corona poling. The poling conditions are 4900V, room temperature, 270 minutes, water drops on the sample, P-P mode.

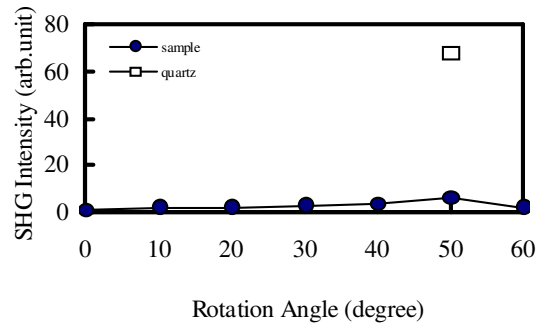


Fig. 11. Experimental results for sample shown in Figure 10 washed by water.

Since this material on the surface can be washed away or destroyed by water, it is clear that SHG intensity can be seen at high temperature because nonlinear region resides not only on the surface but also inside the sample.

4. NLO Effect in SiO₂ Glass by Corona Poling under Salty Environment at 270°C

In this section, we want to find out the relationship between salt water and SiO₂. We prepared the salt-water solution by adding 1g of NaCl into 1000 c.c. of deionized water and put salty water solution drops on glass surface and then performed the corona poling process. Poling time was 270 minutes, temperature was about $270^\circ C$, poling voltage was $4900V$, and distance between sample and the positive electrode needle tip was $1cm$.

The results are shown in Fig. 12. Again we assume that the thicknesses of the depletion layer is $3\mu m$, we obtain (by using the Maker Fringes method):

$$\text{when } l=3\mu m, \quad \frac{I_{2\omega}}{I_\omega^2} = \frac{512\pi^3}{A} \times d_{eff}^2 \times 16.25,$$

$$d_{eff} = 2.52 pm/V.$$

After this experiment, we observed that some residual stains or NaCl like particles seemed to appear on the glass surface. Since Fig. 12 does not show the Maker fringes, so if we used the Maker Fringe method to calculate the d_{ij} value, the value obtained would be too small. This means that the value $d_{eff} =$

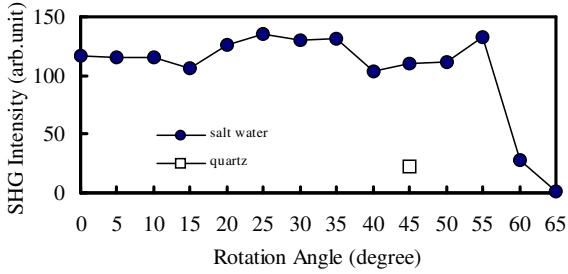


Fig. 12. The NLO effect of glass under corona poling. The poling conditions are 4900V, 270°C, 270 minutes, salt water on the sample, P-P mode.

2.55 pm/V calculated using the Maker Fringe method may be too small for reality. We also calculated the d_{eff}^* used the total intensity method and obtain d_{eff}^* to be 3.99 pm/V. From Fig. 12, we believe that nonlinear region was thicker and more inhomogeneous than those formed under other conditions. After the sample was stored and washed in water for 1 weeks, We could not detect any SHG signal in this sample any more. We can see from Figs. 5 and 12 that the SHG intensity increases when there were salty water drops.

5. NLO Effect in SiO₂ Glass by Corona Poling under Water Vapor Environment at 270°C

In 1992, Okada *et al.* [22] reported that it is charge separation in glass films which caused the observed $\chi^{(2)}$ in Ge-doped optical fibers. Glasses are generally good insulators. Thermally grown amorphous SiO₂ films, for example, have an energy band gap of approximately 8~9 eV, are good insulator. However, defects exist in glass films prepared by rf sputtering. These defects form energy states in between conduction band and valence band, which are associated with trapped electrons. When a strong electric field is applied to a glass film by corona poling, the trapped electrons at defects jump over energy barriers and move to other trap sites. This electron migration occurs in the direction of the electric field and the charges accumulate on one side of the film to set up an internal static electric field E_{in} in the film. This static electric field acts on the third-order optical nonlinearity $\chi^{(3)}$ of the glass film and, as a result, the $\chi^{(2)}$ ($\chi^{(2)} \propto \chi^{(3)} E_{in}$) appears in the film [22].

In 1995, Henry *et al.* [10] reported the optical nonlinearity induced in fused silica through proton implantation. The average $\chi^{(2)}$ is of the order 1 pm/V. In 1996, Takebe *et al.* [16] reported SHG signal from fused silica by corona poling both in air and in vacuum at 280°C. The SHG intensity decreases as the poling time increases in vacuum [16]. These two papers proposed that SHG intensity is related to some defects in fused silica and some ion species in air, such as hydrogen or oxygen ions, during the poling process.

In this experiment we placed the sample in water steam during corona poling at 270°C. We generated the water steam around the sample by heating water in a pot. The result is shown

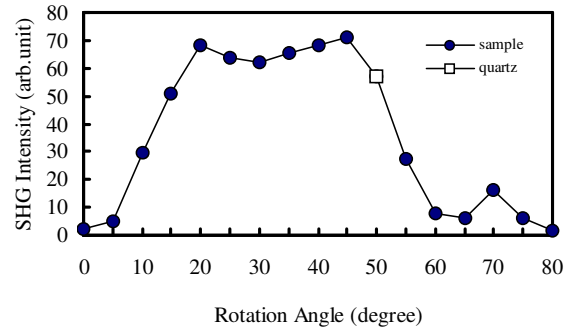


Fig. 13. The NLO effect of glass under corona poling. The poling conditions are 4900V, 270°C, 270minutes, water vapor around the sample, P-P model.

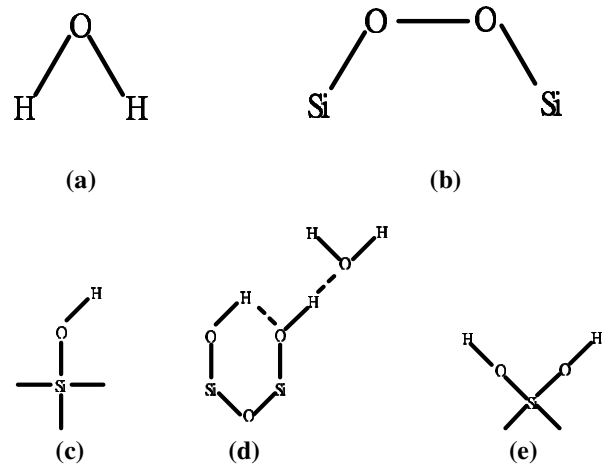


Fig. 14. Schematic diagrams of hydroxyl groups on a silica surface. (a) H₂O. (b) SIOH. (c) Isolated group [9]. (d) Hydrogen-bonded groups with an adsorbed water molecular [9]. (e) Two hydroxyls on one silicon atom [9].

in Fig. 13. If we assume that the nonlinear region thickness is 3 μm thick, then the calculated d_{eff} is almost 1.02 pm/V and d_{eff}^* is 1.64 pm/V. We can see from Figs. 5 and 13 that the SHG intensity increases when there was water vapor. Since Fig. 13 looks very different from Figs. 5, 7, 8, and 10. We speculate that water vapor caused inhomogeneous nonlinear region to form in the sample.

In all the water washing experiment SHG intensity decreases very drastically. When we compared Fig. 5 with Fig. 6, we found that d_{eff} decreases from 0.95 pm/V to 0.076 pm/V. In Figs. 8 and 9, d_{eff} decreases from 0.75 pm/V to 0.42 pm/V. In Figs. 10 and 11, d_{eff} decreases from 1.323 pm/V to 0.305 pm/V. In salt water experiment as shown in Fig. 12, d_{eff} decreases from 2.521 pm/V to 0 pm/V after washing.

We believe that the cations impinged on the sample under high dc field. This phenomenon generates four effects: First, cations impinged on the sample produce defects on sample surface. Second, cations can be implanted into the sample. Third, cations can reacted with SiO₂ or other ions to form new chemical compounds on sample surface. Fourth, cations may form dipole moment not only on the sample surface but also

inside the sample. In general, proton implantation requires high energy. It seemed that our experiment did not employ energy high enough for substantial implantation to occur. The third and fourth effects influenced more than first and second effects. The dipole moments on the sample surface may be due to H_2O (See Fig. 14(a)), and inside the sample may be due to $SiOH$ (See Fig. 14(b)(c)(d).) or SiO_2 [9].

We found that nonlinearity really increases in our samples after poling processes as discussed in this paper, they are somewhat inhomogeneous on the surface or inside the samples. This should be examined in more details by researches in the future.

V. CONCLUSION

We had performed a series of experiments on fused SiO_2 glass samples in this paper. We treated the samples with water, water vapor and salt water during corona poling, SHG intensity from samples were detected. We used the Maker Fringes method to calculate the nonlinear optical coefficients in the SiO_2 samples using a corona poled glass sample as reference. (See Fig. 15.) In our calculation $\chi^{(2)}$ of a corona poled glass sample reference is about $1pm/V$. This is close to the values reported by several other researchers [5,10,19].

We believe that some dipole moments form both on the glass sample surface and near the top surface inside the sample. The impurities cause some dipole moments to form near the surface region inside the sample. In particular, oxygen or hydrogen or other ions obtain energy from corona poling process can form some new chemical compounds both on the glass surface and near the top surface inside the sample. (See Fig. 16.)

We found that when water drop is placed on fused SiO_2 surface during the corona poling, large nonlinearity will be formed in the sample. After the sample is washed in water, SHG intensity decreases drastically. We propose that water, H_2 and some other ions can form hydrogen bonds on the glass surface under the corona poling. These species can be washed away or destroyed by water. We also propose that $SiOH$ is formed inside the fused SiO_2 , it can not be washed away by water easily.

It appears that SHG signal comes more from sample surface than from inside the sample, as is shown clearly in washing experiments in Figs. 6, 9 and 11. The nonlinear materials formed on the surface or inside the sample can lose their nonlinearities by water washing and can even be washed away by water. The SHG intensity in samples decreases very drastically after washing, as shown in all our corona poling experiments under water, water vapor and salty environments. In order for water to reach the nonlinear regions, nanocracks or nanochannels may be formed in the sample so that water can enter the nanocracks and the nanochannels and wash the nonlinear regions.

The thickness of the nonlinear region is about $3 \sim 10\mu m$, formed by corona poling. This small region can contribute large nonlinearity. We tried effectively to increase the strength or the thickness of the nonlinear region by using different corona poling processes under water, water vapour and salty environ-

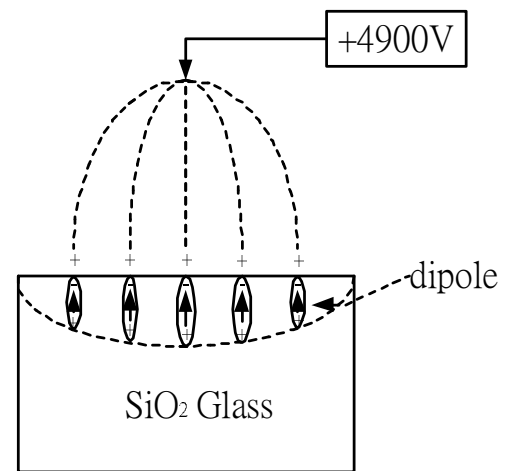


Fig. 15. The dipole moments in SiO_2 glass by corona poling.

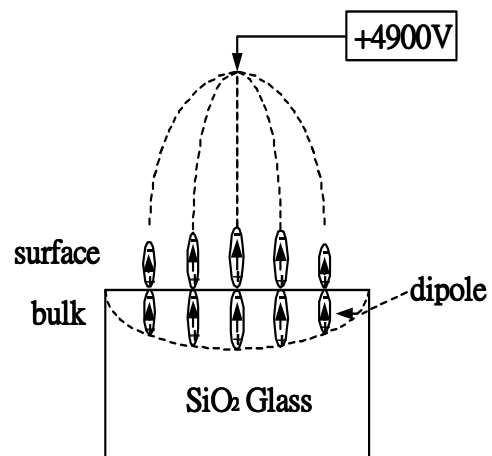


Fig. 16. The dipole moments formed on the surface and inside SiO_2 glass by corona poling in water, salty or water vapor environment.

ments, enhancement effects on nonlinearity in SiO_2 glass were observed. How to further increase the nonlinearity in SiO_2 glass will be an important task in the future.

APPENDIX

Table 1. Sample condition.

Figure 5	(1) The distance between the sample and the positive electrode needle tip is $1cm$. (2) The poling voltage is $4900V$. (3) The temperature was about $270^{\circ}C$. (4) The poling time is about 270 minutes. P-P mode. $d_{eff}=0.95pm/V$.
Figure 6	Experimental results for sample in Figure 5 washed by water. P-P mode. $d_{eff}=0.08pm/V$. $d^*_{eff}=0.10pm/V$
Figure 7	(1) Distance between sample and the positive electrode needle tip is $1cm$. (2) The poling voltage is $4900V$. (3) Experiment temperature was about $270^{\circ}C$. (4) Poling time was 270 minutes. (5) Water

	drops were placed on the surface of glass. P-P mode. $d_{eff}=2.08pm/V$. $d^*_{eff}=1.16pm/V$.
Figure 8	(1) Distance between sample and the positive electrode needle tip is $1cm$. (2) The poling voltage is $4900V$. (3) Experiment temperature was about $270^{\circ}C$. (4) The poling time was 180 minutes. (5) Water drops were placed on glass sample. P-P mode. $d_{eff}=0.70pm/V$. $d^*_{eff}=0.64pm/V$.
Figure 9	Experimental results for sample in Figure 8 washed by water. P-P mode. $d_{eff}=0.42pm/V$ $d^*_{eff}=0.42pm/V$
Figure 10	(1) Distance between the sample and the positive electrode needle tip was $1cm$. (2) The poling voltage is $4900V$. (3) Temperature was room temperature. (4) Poling time was 270 minutes. (5) Water drops were placed on the glass sample surface. P-P mode. $d_{eff}=1.33pm/V$. $d^*_{eff}=1.47pm/V$.
Figure 11	Experimental results for sample in Figure 10 washed by water. P-P mode. $d_{eff}=0.30pm/V$. $d^*_{eff}=0.26pm/V$.
Figure 12	(1) Distance between sample and the positive electrode needle tip is $1cm$. (2) The poling voltage is $4900V$. (3) Experiment temperature was about $270^{\circ}C$. (4) Poling time was 270 minutes. (5) Salty water on glass surface. P-P mode. $d_{eff}=2.52pm/V$. $d^*_{eff}=3.99pm/V$.
Figure 13	(1) Distance between sample and the positive electrode needle tip is $1cm$. (2) The poling voltage is $4900V$. (3) Experiment temperature was about $270^{\circ}C$. (4) Poling time was 270 minutes. (5) Water vapor around the glass sample. P-P mode. $d_{eff}=1.07pm/V$. $d^*_{eff}=1.64pm/V$.

Table 2. Experimental results.

Assume that nonlinear region is about $3\mu m$ thick:

Figure 5	(1) $\theta_{quartz}=45^{\circ}$; $I_{2\omega}=68.1$ (relative arbitrary unit), (2) $\theta_{sample}=40^{\circ}$; $I_{2\omega}=80.8$ (relative arbitrary unit), (3) $n_{\omega}(1.064\mu m)=1.45$, $n_{2\omega}(0.532\mu m)=1.46$ [61], (4) $\begin{cases} \sin \theta = n_{\omega} \sin \theta_{\omega} \\ \sin \theta = n_{2\omega} \sin \theta_{2\omega} \end{cases}$,
----------	---

	$\Rightarrow \begin{cases} \theta_{\omega} = \sin^{-1}(\sin \theta / n_{\omega}) \\ = 26.31^{\circ} \\ \theta_{2\omega} = \sin^{-1}(\sin \theta / n_{2\omega}) \\ = 26.12^{\circ} \end{cases}$
	(5) $t_{\omega} = \frac{2 \cos \theta}{n_{\omega} \cos \theta_{\omega} + \cos \theta} = 0.74$, $T_{2\omega} = 2 \cos \theta_{2\omega} \times n_{2\omega} \times$ $(\cos \theta + n_{\omega} \cos \theta_{\omega}) \times$
	(6) $(n_{\omega} \cos \theta_{\omega} + n_{2\omega} \cos \theta_{2\omega}) \div$ $(n_{2\omega} \cos \theta_{2\omega} + \cos \theta)^3 = 1.58$
	(7) $l_c = \frac{\lambda}{4 n_{\omega} \cos \theta_{\omega} - n_{2\omega} \cos \theta_{2\omega} }$ $= 23.8\mu m$
	(8) $\sin^2 \phi = \sin^2(\frac{\pi l}{2l_c}) = 0.04$,
	(9) $d_{eff} = 0.95 pm/V$.
Figure 6	(1) $\theta_{quartz}=40^{\circ}$; $I_{2\omega}=7.36$ (relative arbitrary unit), (2) $\theta_{sample}=40^{\circ}$; $I_{2\omega}=5.00$ (relative arbitrary unit), (3) $d_{eff}=0.08pm/V$, (4) $lc=23.8\mu m$.
Figure 7	(1) $\theta_{quartz}=50^{\circ}$; $I_{2\omega}=27.1$ (relative arbitrary unit), (2) $\theta_{sample}=50^{\circ}$; $I_{2\omega}=113$ (relative arbitrary unit), (3) $d_{eff}=2.08pm/V$, (4) $lc=22.6\mu m$.
Figure 8	(1) $\theta_{quartz}=50^{\circ}$; $I_{2\omega}=68.0$ (relative arbitrary unit), (2) $\theta_{sample}=45^{\circ}$; $I_{2\omega}=41.5$ (relative arbitrary unit), (3) $d_{eff}=0.70pm/V$, (4) $lc=23.2\mu m$.
Figure 9	(1) $\theta_{quartz}=50^{\circ}$; $I_{2\omega}=68.0$ (relative arbitrary unit), (2) $\theta_{sample}=45^{\circ}$; $I_{2\omega}=13.0$ (relative arbitrary unit), (3) $d_{eff}=0.42pm/V$, (4) $lc=23.2\mu m$.
Figure 10	(1) $\theta_{quartz}=45^{\circ}$; $I_{2\omega}=15.2$ (relative arbitrary unit), (2) $\theta_{sample}=50^{\circ}$; $I_{2\omega}=28.8$ (relative arbitrary unit), (3) $d_{eff}=1.33pm/V$, (4) $lc=22.0\mu m$.
Figure 11	(1) $\theta_{quartz}=50^{\circ}$; $I_{2\omega}=68.0$ (relative arbitrary unit), (2) $\theta_{sample}=50^{\circ}$; $I_{2\omega}=6.08$ (relative arbitrary unit), (3) $d_{eff}=0.30pm/V$, (4) $lc=22.6\mu m$.
Figure 12	(1) $\theta_{quartz}=45^{\circ}$; $I_{2\omega}=23.1$ (relative arbitrary unit), (2) $\theta_{sample}=55^{\circ}$; $I_{2\omega}=133$ (relative arbitrary unit),

	(3) $d_{eff}=2.52\text{pm/V}$, (4) $lc= 21.98 \mu\text{m}$.
Figure 13	(1) $\theta_{\text{quartz}}=50^{\circ}$; $I_{2\omega}=56.9$ (relative arbitrary unit), (2) $\theta_{\text{sample}}=50^{\circ}$; $I_{2\omega}=56.9$ (relative arbitrary unit), (3) $d_{eff}=1.07\text{pm/V}$, (4) $lc= 23.2 \mu\text{m}$.

Table 3. The d_{eff}^* approximate calculation.

	Total intensity from 0° to 60° by $\frac{512\pi^3}{A} I_{\omega}$
Figure 5	123.0 (relative arbitrary unit).
Figure 6	1.407 (relative arbitrary unit).
Figure 7	185.2 (relative arbitrary unit).
Figure 8	56.98 (relative arbitrary unit).
Figure 9	23.03 (relative arbitrary unit).
Figure 10	297.3 (relative arbitrary unit).
Figure 11	9.492 (relative arbitrary unit).
Figure 12	2183.9 (relative arbitrary unit).
Figure 13	368.3 (relative arbitrary unit).
	Approximate d_{eff}^* value:
Figure 5	0.94 pm/V.
Figure 6	0.10 pm/V.
Figure 7	1.16 pm/V.
Figure 8	0.64 pm/V.
Figure 9	0.42 pm/V.
Figure 10	1.47 pm/V.
Figure 11	0.26 pm/V.
Figure 12	3.99 pm/V.
Figure 13	1.64 pm/V.

We used the data for both quartz and sample and calculate $\frac{512\pi^3}{A} I_{\omega}$ for every Figure, then divide the total intensity from 0° to 60° by $\frac{512\pi^3}{A} I_{\omega}$. From equation (11) we used the d_{eff} (Fig. 5) as reference and obtained the approximation effect d_{eff}^* value:

$$d_{eff}^* = d_{(fig.5)} \frac{\sqrt{\text{(total area of SHG)}}}{\sqrt{\text{(total area of SHG in fig.5)}}$$

Assuming nonlinear region is $3 \mu\text{m}$, we used (11) and obtained d_{eff}^* for each figures as listed in Table 3.

REFERENCES

- Aust, J. A., Sanford, N. A. and Amin, J., "Maker fringe analysis of z-cut lithium niobate," *Lasers and Electro-Optics Society Annual Meeting, 1997. LEOS '97 10th Annual Meeting. Conference Proceedings., IEEE*, Vol. 1, pp. 114-115 (1997).
- Bethea, C. G., "Electric field induced second harmonic generation in glass," *Applied Optics*, Vol. 14, pp. 2435-2437 (1975).
- Calvez, A. Le, Freysz, E. and Ducasse, A., "Experimental study of the origin of the second-order nonlinearities induced in thermally poled fused silica," *Optics Letters*, Vol. 22, pp. 1547-1549 (1997).
- Danel, J. S., Dufour, M. and Michel, F., "Application of quartz micro-machining to the realization of a pressure sensor," *IEEE International Frequency Control Symposium*, Vol. 581, pp. 587 - 596 (1993).
- Hall, D. W., Newhouse, M. A., Borelli, N. F., Dumbaugh, W. H. and Weidman, D. L., "Nonlinear optical susceptibilities of high-index glasses," *Applied Physics Letters*, Vol. 54, pp. 1293 (1989).
- Hampsch, H. L. and Torkelson, J. M., "Second harmonic generation in corona poled, doped polymer films as a function of corona processing," *Journal of Applied Physics*, Vol. 67, pp. 1037 (1990).
- Han, K., Lu X., Xu, J., Ma S. and Wang, W., "Second harmonic generation investigation on molecular orientation in Langmuir-Blodgett films poled by an electric field," *Optics Communications*, Vol. 152, pp. 371 (1998).
- Harris, G. L., Jones, E. W., Spencer, M. G. and Jackson, K. H., "Second harmonic conversion in cubic silicon carbide at 1.06 μm ," *Applied Physics Letters*, Vol. 59, pp. 1817 (1991).
- Henry, L. J. and Alan, D. DeVilbiss, "Effect of preannealing on the level of second-harmonic generation and defect sites achieved in poled low-water fused silica," *Journal of Optical Society America B*, Vol. 12, pp. 2037-2045 (1995).
- Henry, L. J., McGrath, B. V., Alley, T. G. and Kester, J., "Optical nonlinearity in fused silica by proton implantation," *Journal of Optical Society America B*, Vol. 13, pp. 827-836 (1995).
- Jerphagnon, J. and Kurtz, S. K., "Maker fringes: a detailed comparison of theory and experiment for isotropic and uniaxial crystals," *Journal of Applied Physics*, Vol. 41, pp. 1667 (1970).
- Kazansky, P. G. and Russel, P. St. J., "Thermally poled glass: frozen-in electric field or oriented dipoles?" *Optics Communications*, Vol. 110, pp. 611-614 (1994).
- Kleinman, D. A., "Nonlinear Dielectric Polarization in Optical Media," *Physical Review*, Vol. 126, pp. 1977 (1962).
- Lundquist, P. M., Ong, H. C., Lin, W. P., Chang, R. P. H., Ketterson, J. B., and Wong, G. K., "Large second-order optical nonlinearities in pulsed laser ablated silicon carbide thin films," *Applied Physics Letters*, Vol. 67, pp. 2919 (1995).
- Maker, P. D., Terhune, R. W., Nisenoff, M., and Savage, C. M., "Effects of dispersion and focusing on the production of optical harmonics," *Physical Review Letters*, Vol. 8, pp. 21-22 (1962).
- Miller, R. C., "Optical second harmonic generation in piezoelectric crystals," *Applied Physics Letters*, Vol. 5, pp. 17 (1964).
- Mukherjee, N., "Dynamics of second-harmonic generation in fused silica," *Journal of Optical Society America B*, Vol. 11, pp. 665-669 (1994).
- Myers, R. A., Mukherjee, N. and Brueck, S. R. J., "Large second-order nonlinearity in poled fused silica," *Optical Letters*, Vol. 16, pp. 1732 -1735 (1991).
- Meyers, R. A., "Large second-order nonlinearity in amorphous SiO2 using temperature/electric-field poling," *The University of New Mexico* (1995).
- Nasu, H., Okamoto, H., Kurashi, K., and Kamiya, K., "Second-harmonic generation from electrically poled SiO2 glasses: effects of OH concentration, defects, and poling conditions," *Journal of Optical Society America B*, Vol. 12, pp. 644-649 (1995).
- Nishikawa, H., Nakamura, R., Tohmon, R., and Ohki, Y., "Generation mechanism of photoinduced paramagnetic centers from preexisting precursors in high-purity silicas," *Physical Review B*, Vol. 41, pp. 7828-7834 (1990).
- Okada, A., Ishii, K., Mito, K., and Sasaki, K., "Phase-matched second-harmonic generation in novel corona poled glass waveguides," *Applied Physics Letters*, Vol. 60, pp. 2853 (1992).
- Okada, A., Ishii, K., Mito, K., and Sasaki, K., "Second-order optical nonlinearity in corona-poled glass films," *Journal of Applied Physics*, Vol. 74, pp. 531 (1993).
- Shen, Y. R., *The Principles of Nonlinear Optic*, John Wiley & Sons, New York, 1984).
- Stagg, J. P., "Drift mobilities of Na^+ and K^+ ions in SiO_2 films," *Applied Physics Letters*, Vol. 31, pp. 532 (1977).
- Takebe, H., Kazansky, P. G., and Russell, P. S. J., "Effect of poling conditions on second-harmonic generation in fused silica," *Optics Letters*, Vol. 21, pp. 468-470 (1996).
- Yariv, A. and Yeh, P., *Optical Waves in Crystals*, 1st ed., John Wiley & Sons, New York, Chap. 7, pp. 220 and Chap. 12, pp. 504 (1983).